

# Influence of Substrate Temperature on the Properties of Fluorinated Silicon-Nitride Thin Films Deposited by IC-RPECVD

J. FANDIÑO,<sup>1,3</sup> A. LÓPEZ-SUÁREZ,<sup>2</sup> B.M. MONROY,<sup>2</sup> G. SANTANA,<sup>2</sup>  
A. ORTIZ,<sup>2</sup> J.C. ALONSO,<sup>2</sup> and A. OLIVER<sup>1</sup>

1.—Instituto de Física, Universidad Nacional Autónoma de México, Coyoacán, 01000 México D.F., AP 20-364, México. 2.—Instituto de Investigaciones en Materiales, Universidad Nacional Autónoma de México, Coyoacán, 04510 México D. F., AP. 70-360, México. 3.—E-mail: jfand72@yahoo.com

Fluorinated silicon-nitride films have been prepared from an Ar/SiF<sub>4</sub>/NH<sub>3</sub> gas mixture by inductively coupled remote plasma-enhanced chemical vapor deposition (IC-RPECVD) at different substrate temperatures, ranging from 150 to 300°C. All of the resulting deposited silicon-nitride films were free of Si-H bonds, showed high dielectric breakdown fields ( $\geq 8 \text{ MV cm}^{-1}$ ), and had root mean square (rms) surface roughness values below 3 Å. The films' refractive indices and the contents of O and F remain constant, but Si/N ratios drop from 5 to 2 and N-H bond concentrations decrease in the range  $(1.3\text{--}0.9) \times 10^{22} \text{ cm}^{-3}$  as the substrate temperature increases. The density of interface states ( $D_{it}$ ) with c-Si was reduced from  $2.4 \times 10^{12}$  to  $8 \times 10^{11} \text{ eV}^{-1} \text{ cm}^{-2}$  at substrate temperatures  $\geq 250^\circ\text{C}$ .

**Key words:** Silicon nitride, PECVD, AFM

## INTRODUCTION

Thin-film silicon nitrides have a wide spectrum of applications in many silicon-based devices and technologies, including solar cells,<sup>1,2</sup> microelectromechanical systems (MEMS),<sup>3</sup> single-electron memories,<sup>4</sup> thin-film transistors (TFTs),<sup>5</sup> integrated optics,<sup>6</sup> and integrated circuits.<sup>7,8</sup> In several of these applications, keeping the deposition temperature of these films in a low range ( $< 400^\circ\text{C}$ ) constitutes a mandatory restriction. For example, the fabrication of a-Si:H TFTs on flexible plastic substrates for large-area imagers and displays requires preparation of silicon-nitride gate dielectrics at temperatures low enough to avoid thermal deformation and/or melting of the substrates.<sup>9</sup> In modern ultra-large-scale integrated (ULSI) circuit technology, where device dimensions continue to shrink,<sup>10</sup> preparation of silicon nitride gate dielectrics at low temperatures is necessary to avoid interdiffusion of elements between adjacent layers or components of the circuit. Use of copper for interconnections in modern deep submicron integrated circuits also requires low-temperature deposition processes to avoid degradation or failure of the copper metalliza-

tion, which may even occur at  $200^\circ\text{C}$ .<sup>11</sup> Plasma-enhanced chemical vapor deposition (PECVD), in different configurations, has been the main technique for depositing silicon-nitride films at low temperatures. Most of the PECVD silicon-nitride films grown using conventional capacitively coupled parallel-plate configuration and SiH<sub>4</sub>/NH<sub>3</sub> and/or SiH<sub>4</sub>/N<sub>2</sub> mixtures have high contents of hydrogen in their networks in the form of Si-H and N-H bonds. The hydrogen content in these films usually increases, and their properties deteriorate, as the deposition temperature decreases.<sup>12,13</sup>

Substituting the conventional plasma sources by high-density plasma sources (HDPS) along with the use of the conventional reactive gas sources has proved to be effective for reducing the hydrogen content in silicon-nitride films deposited at substrate temperatures lower than  $400^\circ\text{C}$ .<sup>14</sup> Another way to face the problem of H incorporation in the films involves changing of the traditional silicon gaseous source by other sources with fewer (or no) H atoms per Si atom, such as SiCl<sub>2</sub>H<sub>2</sub>, SiCl<sub>4</sub>, and SiF<sub>4</sub>. Some recent works have shown that use of SiF<sub>4</sub>/NH<sub>3</sub> mixtures in combination with HDPS allows the deposition of fluorinated silicon-nitride films, which contain a reduced amount of N-H bonds and are completely free of Si-H bonds, even at temperatures

(Received July 21, 2005; accepted February 8, 2006)

as low as 350°C or 250°C.<sup>15,16</sup> Despite the fact that some previous works have shown that the substrate temperature has important effects on the surface reactivity of SiF<sub>x</sub> radicals in fluorosilane plasmas,<sup>17</sup> the effect of the substrate temperature on the properties of fluorinated silicon-nitride films has not been thoroughly investigated.

In this work, the structural and electrical properties of the fluorinated silicon-nitride films obtained from an Ar/SiF<sub>4</sub>/NH<sub>3</sub> mixture by IC-RPECVD were investigated as a function of the deposition temperature in the range from 150°C to 300°C. Because one possible application of these films is as gate dielectrics in metal-insulator-crystalline silicon field-effect transistors (MISFET), special interest was put in investigating the effect of the substrate temperature on the current-voltage (I-V) and capacitance-voltage (C-V) characteristics and the density of interface states (D<sub>it</sub>) of the films as part of MIS capacitors.

### EXPERIMENTAL DETAILS

The fluorinated silicon-nitride films grown for this study were deposited in an IC-RPECVD system that has been previously described.<sup>16</sup> Ultra-high-purity Ar (99.999%, Praxair Mexico, Mexico) and NH<sub>3</sub> (99.999%, Praxair) were fed into the plasma zone from the top end of the system, while SiF<sub>4</sub> (99.99%, Praxair) was fed downstream of the plasma by means of one dispersal ring.

All deposition parameters were kept constant, as can be seen in Table I, except for the substrate temperature, which was varied between 150°C and 300°C. For structural characterization, films of ~400 nm were grown on n-type crystalline <100> silicon substrates of 200 Ω cm and then cut into 1.5 cm × 1.5 cm pieces. These substrates were cleaned with an aqueous solution of diluted HF prior to being loaded into the chamber. Thickness and refractive index of the films were measured by null-/single-wavelength ellipsometry, using a Gaertner L117 ellipsometer (λ = 632.8 nm). Chemical-bond analysis was performed with the aid of a FTIR Nicolet 210 spectrophotometer in a wavenumber range of 400–4000 cm<sup>-1</sup> with 8-cm<sup>-1</sup> resolution in order to avoid interference effects. Atomic composition of the films was assessed by means of Rutherford backscattering spectrometry (RBS) measurements, carried out in the Instituto de Física 3MV 9SDH-2 Pelletron accelerator using a colli-

dated 3.045-MeV α particle beam with 2-mm diameter, 0.1-μA ion current, and a beam charge of 200 μC. Backscattered particles were collected at 168° with an Oxford 50-11 surface barrier detector. Accurate film thickness measurements (provided by ellipsometry) together with RBS data were used in order to obtain information about film densities. Atomic force microscopy (AFM) images were recorded with a JEOL JSPM-4210/TM-4210BU scanning probe microscope, using MikroMasch DP15/HIRES/AIBS/15 high-resolution probes in tapping mode.

In order to perform the electrical characterization of the films, metal-insulator-semiconductor (MIS) capacitors were constructed by depositing silicon-nitride films of approximately 90 nm in thickness on 1.0-Ω cm resistivity n-type crystalline <100> silicon substrates, and the original (2-in. diameter) wafers were cut into four sections. Al dots (0.013 cm<sup>2</sup> in area and 100 nm thick) were then thermally evaporated through a metallic mask onto the silicon-nitride film surface, to define the MIS capacitors. As a back ohmic contact, we used an In-Ga eutectic alloy, applied manually with a small applicator onto the silicon substrate. Approximately 50 devices per substrate were constructed. Before film deposition, the low-resistivity substrates used to prepare the MIS capacitors were subjected to a standard ex-situ RCA cleaning procedure and then to an in-situ surface pretreatment by means of NH<sub>3</sub> plasma at 130 W and 56 mtorr for 2.5 min. at room temperature. As has been reported earlier, the purpose of NH<sub>3</sub> plasma surface treatment is to improve the silicon-nitride/silicon interface by the nitridation and/or reconstruction of the silicon surface.<sup>18,19</sup> It is worth mentioning that in some preliminary experiments, MIS capacitors were constructed using films prepared under the same deposition conditions used in this work, but without the NH<sub>3</sub> plasma treatment of the silicon substrates, and no quasi-static C-V curve could be measured due to the very high values of the density of states and leakage currents (Q/t). This gave experimental evidence for the necessity of improvement and/or modification of the silicon surface for obtaining reasonable low values of the density of interface states. Although a more detailed study on the NH<sub>3</sub> plasma parameters (pressure, RF power, temperature, and time) to optimize the improvement of the silicon surface quality is underway, after some trial-and-error tests with the NH<sub>3</sub> plasma pretreatments, we found the surface pretreatment conditions mentioned before gave reasonable low values of Q/t, to make possible the investigation of the effect of substrate temperature on the silicon nitride/silicon interface.

Current-voltage characteristics of the MIS capacitors were assessed at 0.5 V s<sup>-1</sup> with the aid of a Keithley 230 voltage source and a Keithley 485 picoammeter controlled through the IEEE-488 bus via software. Simultaneous high- and low-frequency capacitance vs. voltage (C-V) measurements were

Table I. Growth Parameters Used in This Study

Parameter	Units	Value
Ar flow rate	sccm	37.0
SiF <sub>4</sub> flow rate	sccm	1.5
NH <sub>3</sub> flow rate	sccm	7.0
Pressure	mtorr	10
RF power	watts	550
Temperature	°C	150, 200, 250, 300

performed using a Keithley Model 82 simultaneous C-V system.

## RESULTS AND DISCUSSION

### Composition and Structural Characterization

The atomic percentages of Si, N, F, and O in the films obtained by the simulation of the experimental RBS spectra using the SIMNRA code<sup>20</sup> are presented in Fig. 1 as a function of the substrate temperature. As can be seen, all the films are silicon-rich since the concentration of Si atoms is higher than that of N atoms. The composition is nearly constant for films deposited at temperatures in the range from 200°C to 300°C, but the Si concentration increases and the amount of N and F decreases when the substrate temperature is 150°C. These results can be explained in terms of the deposition mechanisms proposed previously for the growth of silicon-nitride films from  $\text{SiF}_4/\text{NH}_3$  plasmas.<sup>16</sup> According to this model, the silicon-nitride films grow from reactions between mainly SiF and NH radicals, and consequently, it is natural that some Si-F and N-H bonds remain in their network. Because the strength of the Si-F bonds is higher than that of the N-H bonds,<sup>21,22</sup> it is expected that the amount of Si-F bonds incorporated in the films be larger than the amount of N-H bonds, which explains the silicon-rich composition of the films. The increase of the Si/N ratio at low substrate temperature can be explained in terms of changes in the condensation rate and surface reactivity of  $\text{SiF}_x$  ( $x = 1, 2, 3$ ) radicals, similar to those occurring in  $\text{SiF}_4$  and  $\text{SiF}_4:\text{H}_2$  plasmas.<sup>17</sup> According to this, at low enough substrate temperatures ( $\leq 150^\circ\text{C}$  in this case), an increase in the condensation rate of volatile radicals such as  $\text{SiF}_2$ ,  $\text{SiF}_3$ , and  $\text{NH}_2$ , is expected. These can react between them on the substrate surface to form other volatile compounds,

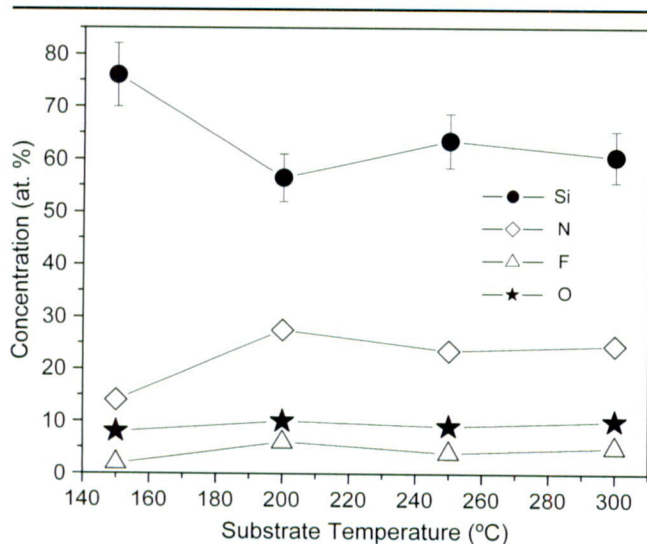


Fig. 1. Film composition as a function of substrate temperature obtained from RBS.

such as  $\text{NF}_3$ ,  $\text{H}_2$ ,  $\text{HF}$ , etc. The occurrence of these reactions, along with the surface heterogeneous reactions that form the solid film, gives rise to the removal of N and F from the growing film, which leaves a film with a more silicon-rich composition. The removal of N and F atoms from the growing film can also generate an important amount of dangling silicon bonds in the film network. The incorporation of oxygen in the films can be explained as a result of a post-deposition oxidation process generated by the exposure of the films to the ambient atmosphere. The occurrence of this oxidation process is indicative of films with a relatively open structure and/or with a considerable amount of dangling bonds in their network.<sup>23</sup> These composition and structural results are consistent with values and behavior of the refractive index and density of the films as a function of substrate temperature ( $T_S$ ), shown in Fig. 2. As can be seen from this figure, both parameters behave similarly with respect to  $T_S$ , i.e., they are practically constant for films deposited at substrate temperatures  $\geq 200^\circ\text{C}$  and decrease for the film deposited at  $150^\circ\text{C}$ . The low density of the films compared to the ideal silicon-nitride material ( $3.1 \text{ g cm}^{-3}$ ) confirms the open structure of the films and/or the presence of dangling bonds. On the other hand, the low density of the films, along with the incorporation of O and F in their network, also explains why the refractive index of the films is lower than that of the stoichiometric silicon nitride ( $n = 2.00$ ), despite the fact that they are silicon-rich.<sup>16,23</sup>

It is worth mentioning that the decreases in film refractive index and density as the substrate temperature is decreased are more noticeable in silicon-nitride films prepared from  $\text{SiH}_4/\text{NH}_3$  discharges.<sup>13,14</sup> According to our model for film growth, the reason for these differences may be that both the rate of condensation and the reactivity of the  $\text{SiH}_x$  radicals are more sensitive to the substrate temperature than are those of  $\text{SiF}_x$  radicals.

Figure 3 shows the infrared spectra of the films, with the deposition temperature as a parameter.

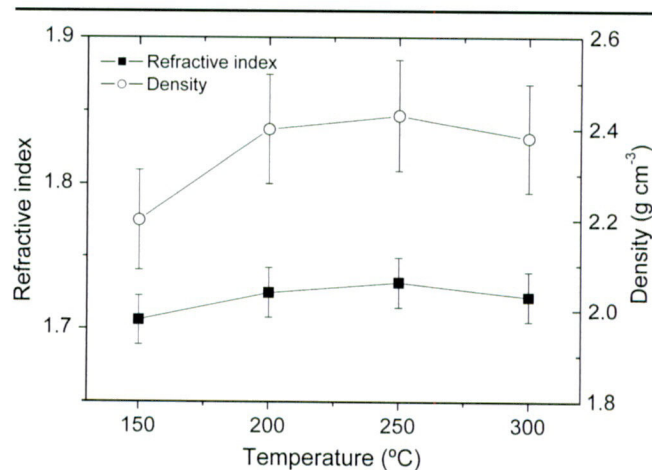


Fig. 2. Density and refractive index behavior as a function of substrate temperature.

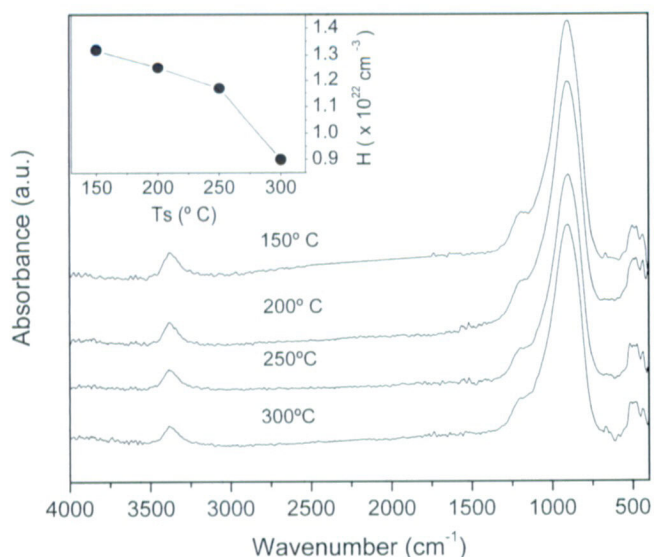


Fig. 3. FTIR spectra of the films. (Inset) N-H bond concentration as a function of substrate temperature, calculated from Eq. 1.

The broad band centered at  $902\text{ cm}^{-1}$  corresponds to Si-N stretching vibrations shifted from their original position ( $\sim 850\text{ cm}^{-1}$ ) due to F incorporation in the film network. Absorption peaks at  $3,380$  and  $1,213\text{ cm}^{-1}$  are related to N-H stretching and bending modes, respectively, and the band centered at  $\sim 500\text{ cm}^{-1}$  can be assigned to a Si-N bending mode. No evidence of Si-H absorption ( $\sim 2,170\text{ cm}^{-1}$ ) was found over the entire range of substrate temperatures investigated.

A slight decrease in the N-H stretching peak is observed in the FTIR spectrum (Fig. 3) as the substrate temperature increases from  $150$  to  $300^\circ\text{C}$ . In order to quantify this change, the N-H bond concentrations (in  $\text{cm}^{-3}$ ) were calculated using the equation

$$C_{\text{N-H}} = A \int \frac{\alpha(\nu)}{\nu} d\nu \quad (1)$$

where  $A$  is a constant equal to  $2.8 \times 10^{20}\text{ cm}^{-2}$  for N-H bonds and the integral must be taken through all the wavenumbers ( $\nu$ ) included in the peak centered at  $3,380\text{ cm}^{-1}$ .

The results obtained from these calculations are plotted (inset, Fig. 3) vs. substrate temperature, where a monotonic decrease in N-H bond concentration (which is equal to the H concentration because no Si-H bonds are present) is observed as the substrate temperature rises. This behavior could be explained in terms of a reduction in the residence time of H-related species on the growing film surface as the temperature increases.

The stability of the samples under exposure to ambient air and moisture was systematically studied by recording IR transmission spectra and measuring refractive indices after different intervals of time. No changes were detected in the IR characteristics or in the refractive index of any of the samples, even after 1 mo.

AFM images of  $4\text{ }\mu\text{m} \times 4\text{ }\mu\text{m}$  portions of the film surfaces are shown in Fig. 4 for all substrate temperatures studied. The films have small surface features, typical of amorphous materials. Because the top of the height ( $z$ ) scale is set at  $\sim 2.6\text{ nm}$  in all cases, very smooth films surface are expected. The root mean-squared roughness ( $R$ ) values were calculated from the AFM images (Fig. 4), and the results are shown in Table II. All the films have  $R$  values lower than those reported for PECVD silicon-nitrides deposited from  $\text{SiH}_4$ -based mixtures<sup>24–26</sup> and are similar to the values reported for LPCVD silicon nitrides grown at  $700^\circ\text{C}$ .<sup>24</sup> A number of factors, such as sticking coefficients, surface chemical reactions, ion bombardment, surface diffusion, etc., directly influence the growth of the film.<sup>27,28</sup> In our case, given the high plasma power condition used for deposition, we believe that the enhancement of surface diffusion by ion bombardment was the key factor for obtaining the smooth surfaces.

### Electrical Behavior

Current density vs. electric field curves of the MIS capacitors for different substrate temperatures are

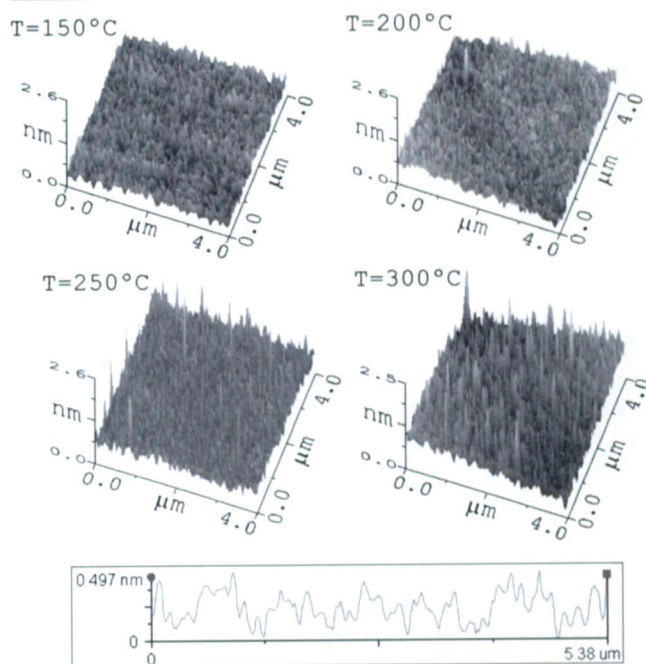


Fig. 4. AFM images of fluorinated silicon-nitride films deposited at different substrate temperatures. A line-scanning plot (lower plot) for one of the films ( $T_s = 150^\circ\text{C}$ ) is included.

Table II. Root Mean Square Roughness of Film Surface as a Function of Substrate Temperature

Substrate Temperature ( $^\circ\text{C}$ )	RMS Roughness ( $\text{\AA}$ )
150	1
200	1
250	1
300	2

shown in Fig. 5. All the curves have similar shape and are characterized by a low leakage current density for electric fields up to  $5 \text{ MV cm}^{-1}$ .

We define the dielectric breakdown field ( $E_B$ ) as the electric field needed to produce a current of 1 mA across the sample. The best 20 devices per wafer were used in order to report an average value of  $E_B$ . Breakdown fields of  $\sim 8\text{--}9 \text{ MV cm}^{-1}$  are achieved for all of the MIS capacitors. These high values of  $E_B$  are expected due to the stronger nature of the Si-F bonds compared to Si-N bonds and the absence of weak Si-H bonds in the silicon-nitride network through the entire  $T_S$  range investigated.

Simultaneous C-V curves of the constructed MIS capacitors were measured, and the results obtained are illustrated in Fig. 6 for different substrate temperatures.

All of the C-V curves in Fig. 6 appear shifted to negative voltage values with respect to the ideal MIS capacitor, indicating the presence of a positive

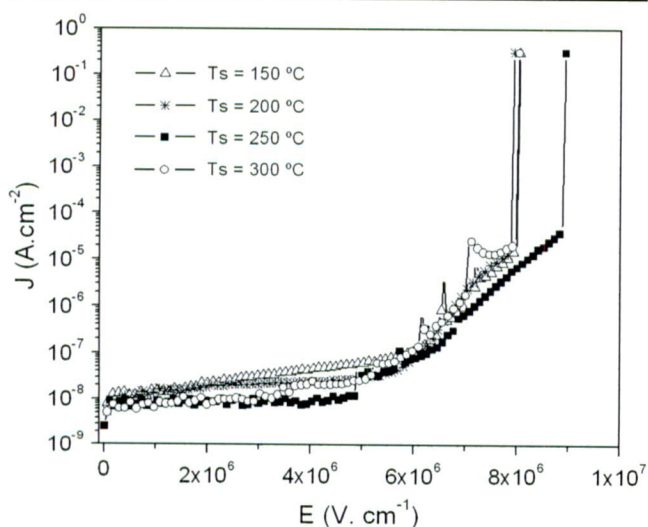


Fig. 5.  $J$  vs.  $E$  plots with the substrate temperature as a parameter.

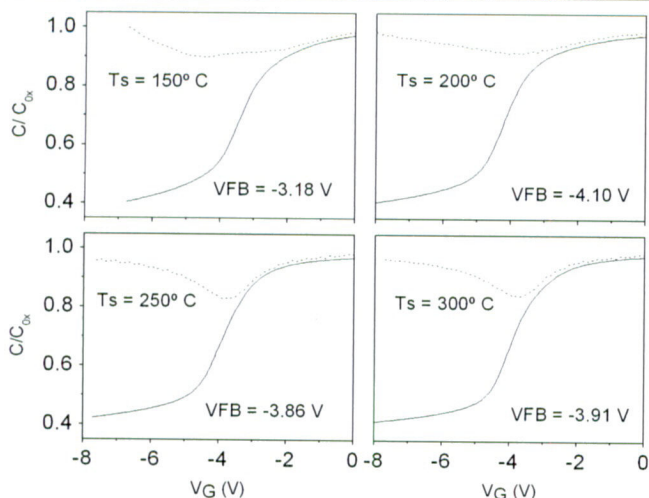


Fig. 6. Simultaneous C-V plots for different substrate temperatures, where the continuous line represents the high-frequency capacitance, the discontinuous line accounts for quasi-static capacitance, and  $V_{FB}$  is the flat-band voltage.

charge density in the gate dielectric films. In agreement with the observed behavior, flat-band voltage lies between  $-3$  and  $-4 \text{ V}$  in all cases. Also, the shape of the quasi-static C-V curves improves when the substrate temperature increases above  $250^\circ\text{C}$ .

The density of interface states ( $D_{it}$ ) values were calculated with the aid of both high-frequency and quasi-static C-V measurements.<sup>29</sup> The  $D_{it}$  state values at midgap ( $D_{it}(0)$ ) are plotted in Fig. 7 as a function of substrate temperature. In general, those values are in the moderate to high range and agree with previous reports for PECVD silicon-nitride-based MIS structures.<sup>26</sup> The  $D_{it}(0)$  vs.  $T_S$  curve follows nearly constant behavior from  $150$  to  $200^\circ\text{C}$ , drops from  $200^\circ\text{C}$  to  $250^\circ\text{C}$ , and then remains approximately constant up to  $300^\circ\text{C}$ . At present, this behavior is not fully understood, but it could be related to the temperature dependence of the surface mobility and/or reactivity of the  $\text{SiF}_x$  and  $\text{NH}_y$  species adsorbed on the substrate surface in the initial stage of film growth and the ability of these species to passivate the dangling bonds that are present on the substrate surface.

## CONCLUSIONS

Fluorinated silicon-nitride films were deposited by IC-RPECVD using an  $\text{Ar}/\text{SiF}_4/\text{NH}_3$  mixture after the substrates were treated by a  $\text{NH}_3$  plasma. Structural and electrical properties of the films were investigated as a function of substrate temperature in the range between  $150^\circ\text{C}$  and  $300^\circ\text{C}$ . All of the films were Si-H bond free up to the FTIR detection limit. Substrate temperature has little influence on film composition above  $200^\circ\text{C}$  but causes a monotonic decrease in H content when the temperature increases through the entire range. High dielectric breakdown fields ( $8\text{--}9 \text{ MV cm}^{-1}$ ) were achieved in all cases. The density of states at dielectric/semiconductor interface improves when substrate temperature

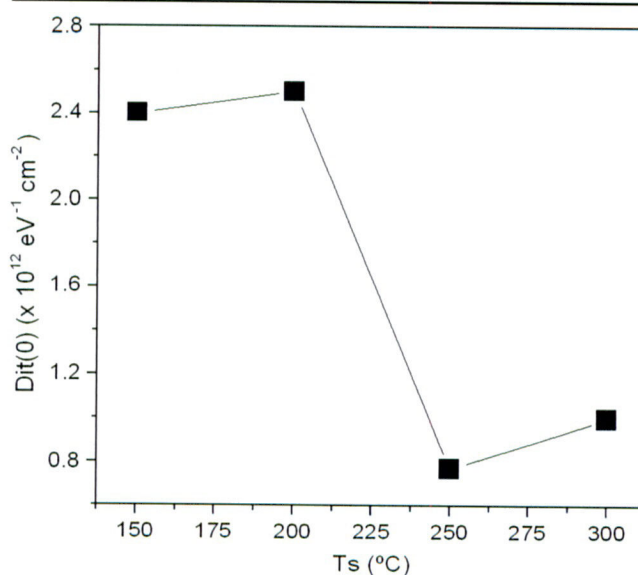


Fig. 7. Density of states at midgap vs. substrate temperature.

surpasses 250°C. Very smooth surfaces, with the lowest rms R values reported for as-grown PECVD silicon-nitride films (1–2 Å), were obtained regardless of substrate temperature.

### ACKNOWLEDGEMENTS

The authors thank C. Flores and M. Canseco from the Instituto de Investigaciones en Materiales UNAM for technical assistance with AFM and FTIR measurements and K. López and F.J. Jaimes from the Instituto de Física UNAM for technical assistance with the Pelletron accelerator. This work has been partially supported by CONACyT-México under project 47303-F.

### REFERENCES

1. A. Hauser, M. Spiegel, P. Fath, and E. Bucher, *Solar Energy Mater. Sol. Cells* 75, 357 (2003).
2. I.O. Parm, K. Kim, D.G. Lim, J.H. Lee, J.H. Heo, J. Kim, D.S. Kim, S.H. Lee, and J. Yi, *Solar Energy Mater. Sol. Cells* 74, 97 (2002).
3. G. Caliano, F. Galanello, A. Caronti, R. Carotenuto, M. Pappalardo, V. Foglietti, and N. Lamberti, 2000 IEEE Ultrasonics Symposium (Piscataway, NJ: IEEE, 2000), p. 963.
4. H. Sunamura, T. Sakamoto, Y. Nakamura, J.S. Tsai, and T. Baba, *Appl. Phys. Lett.* 74 (3), 3555 (1999).
5. G. Lavareda, C. Nunes de Carvalho, A. Amaral, E. Fortunato, A.R. Ramos, and M.F. Da Silva, *Thin Solid Films* 427, 71 (2003).
6. T. Naganawa, H. Haeiwa, and Y. Kokubun, *Jpn. J. Appl. Phys.* 43, 5780 (2004).
7. K. Sekine, Y. Saito, M. Hirayama, and T. Ohmi, *J. Vac. Sci. Technol., A* 17 (5), 3129 (1999).
8. R.B. Beck, M. Giedz, A. Wojtkiewicz, A. Kudla, and A. Jakubowski, *Vacuum* 70, 323 (2003).
9. A. Sazonov and C. McArthur, *J. Vac. Sci. Technol., A* 22 (5), 2052 (2004).
10. M.R. Wang, M.B. Yu. Rusli, N. Babu, C.Y. Li, and K. Rakesh, *Thin Solid Films* 462–263, 219 (2004).
11. H.C. Kim and T.L. Alford, *Thin Solid Films* 449, 6 (2004).
12. M.T.K. Soh, N. Savvides, C.A. Musca, M.P. Martyniuk, and L. Faraone, *J. Appl. Phys.* 97, 093714 (2005).
13. B.A. Walmsley, Y. Liu, X.Z. Hu, M.B. Bush, K.J. Winchester, M. Martyniuk, J.M. Dell, and L. Faraone, *J. Appl. Phys.* 98, 044904 (2005).
14. J. Yota, J. Hander, and A.A. Saleh, *J. Vac. Sci. Technol., A* 18 (2), 372 (2000).
15. H. Otha, M. Hori, and T. Goto, *J. Appl. Phys.* 90 (4), 1955 (2001).
16. J. Fandiño, A. Ortiz, L. Rodríguez-Fernández, and J.C. Alonso, *J. Vac. Sci. Technol., A* 22 (3), 570 (2004).
17. K.L. Williams and E.R. Fisher, *J. Vac. Sci. Technol., A* 21 (4), 1024 (2003).
18. M. Bose, D.K. Basa, and D.N. Bose, *Mater. Lett.* 48, 336 (2001).
19. G. Lukovsky, S.S. Kim, and J.T. Fitch, *J. Vac. Sci. Technol., B* 8, 822 (1990).
20. M. Mayer, *SIMNRA User's Guide*, Version 4.4 (Garching, Germany: Max Planck-Institute für Plasmaphysik, 1997).
21. R.T. Sanderson, *Chemical Bonds and Bond Energy*, 2nd ed. (New York: Academic Press, 1976), pp. 103–147.
22. J.A. Kerr and D.W. Stockes, "Strengths of Chemical Bonds," in *Handbook of Chemistry and Physics*, D.R. Lide, ed.-in-chief, 83rd ed. (Boca Raton: Academic Press, 2002–2003), pp. 9.52–9.75.
23. J. Fandiño, G. Santana, L. Rodríguez-Fernández, J.C. Cheang-Wong, A. Ortiz, and J.C. Alonso, *J. Vac. Sci. Technol., A* 23 (2), 248 (2005).
24. G.R. Yang, Y.P. Zhao, Y.Z. Hu, T.P. Chow, and R.J. Gutmann, *Thin Solid Films* 333, 219 (1998).
25. A. Amassian, R. Vernhes, J.E. Klemberg-Sapieha, P. Desjardins, and L. Martinu, *Thin Solid Films* 469–470, 47 (2004).
26. Y. Park and S. Rhee, *J. Mater. Sci.: Mater. Electron.* 12, 515 (2001).
27. T. Karabacak, Y.P. Zhao, G.C. Wang, and T.M. Lu, *Phys. Rev. B: Condens. Matter Mater. Phys.* 66, 075329 (2002).
28. W. Xu, B. Li, T. Fujimoto, and I. Kojima, *Surf. Coat. Technol.* 135, 274 (2001).
29. E.H. Nicollian and J.R. Brews, *MOS (Metal Oxide Semiconductor) Physics and Technology* (New York: John Wiley & Sons, 1982), pp. 319–370.